

STATUS OF GLOBAL QCD ANALYSIS AND THE PARTON STRUCTURE OF THE NUCLEON

WU-KI TUNG

*Michigan State University, E. Lansing, MI, USA**E-mail: Tung@pa.msu.edu*

The current status of global QCD analysis of parton distribution functions of the nucleon is reviewed. Recent progress made in determining various features of the parton structure of the nucleon, as well as outstanding open questions are discussed. These include: the small- x and large- x behavior of the partons, particularly the gluon; the differentiation of u and d quarks; the strangeness sea ($s + \bar{s}$), the strangeness asymmetry ($s - \bar{s}$); and the heavy quark distributions c and b . Important issues about assessing the uncertainties of parton distributions and their physical predictions are considered. These developments are all critical for the physics programs of HERA II, Tevatron Run II, RHIC, and LHC.

This talk is devoted to a review of the present status of global QCD analysis of parton distribution functions (PDFs) of the nucleon. Progress on global QCD analysis of PDFs depends on continued advancement in experimental inputs from a variety of hard processes, in theoretical development (such as higher-order calculations and resummation techniques), and in analysis methodology (such as statistical techniques and uncertainty assessment). Significant developments on all these fronts have been taking place. Since both precision standard model (SM) phenomenology and beyond SM “new physics” searches depend on reliable knowledge of PDFs, continued progress on global QCD analysis of PDFs is vital for the physics programs of HERA II, Tevatron Run II, RHIC, and LHC.

2004 marks the 20th anniversary of two landmark works in the field of PDF analysis—that of Duke-Owens [1] and Eichten-Hinchliffe-Lane-Quigg [2]. It seems appropriate to present this review from the historical perspective, assessing the impressive progress that has been made during the intervening years, as well as emphasizing the many open problems that remain to be addressed and resolved. We shall see that in order to meet the challenges of collider physics in the coming decade, the unfinished tasks in global QCD analysis continue to be extremely demanding on all fronts.

Due to space limitations, only a few key references are given. Detailed references to the original literature can be found in various review articles and on the web pages of the experimental and PDF analysis groups to be mentioned in the ensuing sections.

1 Progress in Global QCD Analysis

Historically, structure functions in deep inelastic scattering (DIS) of leptons on hadrons, measured in fixed target experiments, provided the first significant experimental inputs to PDF analysis. They allowed the first determination of the u , d and singlet quark distributions, as well as the general behavior of the gluon distributions, indirectly through QCD evolution and sum rules. Lepton-pair production in hadron collisions (Drell-Yan process) provided dramatic confirmation of the universality of these PDFs, and furnished critical constraints on the sea quark distributions \bar{u} and \bar{d} , thus allowing a meaningful separation of the valence distributions u_{val} , d_{val} from the (total) u , d distributions.

Successive generations of DIS experiments, with a variety of lepton beams ($e^\pm, u^\pm, \nu, \bar{\nu}$) and hadron targets (p, D, A), allowed better separation of d from u and the valence from the sea distributions. The $(\bar{d} - \bar{u})$ difference was found to be non-zero, i.e. the sea partons are not flavor-blind. (This vitiated the Gottfried sum rule.) The measurement of the pD to pp Drell-Yan cross section ratio provided critical information that dramatically altered the behavior of the extracted \bar{d}/\bar{u} ratio of parton distributions. Complementary to this, the measurement of the forward/backward asymmetry of the lepton rapidity distribution in W -production (or, equivalently, the W^+/W^- ratio) at the Tevatron provided valuable constraints on the d/u ratio.

The HERA experiments, H1 and ZEUS, greatly expanded the kinematic range over which the DIS structure functions are measured, especially for small x , and elevated the precision of these measurements to

unprecedented levels. These advances not only pinned down certain combinations of the quark distributions to a high degree of accuracy, but also allowed better determination of the gluon distribution $g(x, Q)$ through the much improved measurement of the Q -dependence of the structure functions. Combined with direct constraints provided by inclusive jet production measurements in hadron-hadron collisions (by the CDF and D0 experiments) at medium to large x , we now have a far better picture of the gluon distribution than a few years ago. Nonetheless, the relative uncertainty on $g(x, Q)$ compared to the quark distributions is still large.

At the highest Q values reached at HERA, structure functions due to W^\pm (charged current) exchange and $Z\gamma$ interference (neutral current) have also been measured. They provide dramatic confirmation of the SM formalism, as well as new opportunities to cleanly differentiate the u and d quarks. (Current analyses, based on DIS on deuteron or nuclear targets, are sensitive to model-dependent nuclear corrections). However, due to the small cross section at large Q , the accuracy of current measurements is limited. So far, one can only verify that existing PDFs agree with available high Q CC and NC HERA data.

The differentiation of strange quark distributions from non-strange ones can, in principle, be obtained as differences in totally inclusive structure functions from neutral-current (NC) and charged-current (CC) DIS experiments. But the systematic uncertainties for such analysis is too large to make this method reliable. Instead, one has to rely on the semi-inclusive measurement of charm production in neutrino (and anti-neutrino) scattering. All evidence from these measurements points to suppressed s and \bar{s} distributions inside the nucleon compared to the non-strangeness sea quarks [say, $\frac{1}{2}(\bar{u} + \bar{d})$] by a factor of roughly $\frac{1}{2}$ at the confinement scale of order $Q \sim 1$ GeV. This result has been incorporated in existing global analyses as an overall constant factor. More detailed analysis of the strangeness sector, including the shapes of s and \bar{s} distributions and possible differences between them has just begun recently, as will be described in Sec.1.

In addition to the “light partons,” we also need to understand the partonic structure of the nucleon in the heavy flavor sectors, particularly c and b —for their intrinsic importance, as well as their influence on processes such as top and Higgs production. All phenomenological work, so far, assumes “radiatively generated” heavy flavors—the (c, b, t) partons are generated by QCD evolution without a non-perturbative component at the respective heavy flavor threshold. This is not a satisfactory situation because the “heavy flavor threshold” is not a well-defined PQCD concept (any value of the same order of magnitude as the heavy quark mass is acceptable). A zero value for the heavy quark distribution at one threshold value would imply non-zero values at other possible choices for the threshold. Nonetheless, the PQCD formalism for treating heavy flavor partons has developed steadily in the last ten years. Quantitative, systematic phenomenological work is only at an early development stage. To make substantial progress, more data on heavy flavor production from a variety of processes will be needed.

Historical Development

To gain a historical perspective on the progress of our knowledge of the parton structure of the nucleon, we start with Table I, which shows how a sequence of representative historical PDFs fare when they are compared with the currently available high precision data. This comparison is meant to show the broad historical trend, thereby to give a semi-quantitative measure of the progress that has been made through these years. To this end, we convolute these PDF sets, in turn, with the *same* set of hard cross sections (that used in the CTEQ global analysis); compute the χ^2 values for the various processes; then examine the results. This procedure inevitably involves some mismatch between the PDFs and the hard cross sections for PDF sets obtained by other groups (such as MRST and GRV) because of differences in the choice of schemes and prescriptions for calculating hard cross sections. To emphasize the historical trend only, we group the PDF sets by periods and average over the sets from various groups in the last column, which carries the main message. (The numbers in adjacent rows within each group should not be taken literally as measures of relative merit.) By this account, the accuracy of PDFs has improved steadily, by a factor of ten over these years. The impact of second generation fixed-target DIS experiments (BCDMS, NMC, CCFR), $e\text{-}p$ collider experiments (H1, ZEUS), and the addition of DY-W production experiments, and jet inclusive production experiments (CDF, D0), recounted in the first part of this section, all contribute noticeably in the progression of improvements. We next survey the influence of these developments on the behavior of the various PDFs themselves.

The u and d distributions:

The two graphs in Fig.(1) show the historical evolution of the u and d distributions at $Q^2 = 10$ GeV 2 .

| | Time period | Fixed-tgt | HERA | DY-W | Jets | Total | χ^2/pt |
|------------|-------------|-----------|-------|------|------|-------|--------------------|
| # data pts | | 1070 | 588 | 145 | 123 | 1926 | |
| EHLQ | 1984 | 6255 | 20734 | 3088 | 328 | 30405 | 12.9 |
| DuOw | | 3636 | 12572 | 2705 | 273 | 19186 | |
| MoTu | 1990 | 3551 | 11881 | 857 | 218 | 16508 | 11.0 |
| KMRS | | 1816 | 23205 | 577 | 280 | 25877 | |
| CTQ2M | 1994 | 1530 | 2096 | 646 | 224 | 4497 | 3.0 |
| MRSA | | 1590 | 1327 | 249 | 231 | 3397 | |
| GRV94 | | 1496 | 7295 | 302 | 213 | 9306 | |
| CTQ4M | 1998 | 1415 | 797 | 227 | 206 | 2645 | 1.4 |
| MRS981 | | 1399 | 1007 | 111 | 227 | 2744 | |
| CTQ6M1 | 2001-02 | 1239 | 611 | 159 | 123 | 2132 | 1.2 |
| MRST01 | | 1378 | 714 | 120 | 236 | 2448 | |

Table 1. Historical PDFs evaluated on current data sets in the \overline{MS} scheme, to show the steady progress that has been made in determining the parton structure of the nucleon. Focus is on the historic trend, particularly illustrated by the last column, rather than on detailed numbers in neighboring rows, which are subject to various caveats. (See text.)

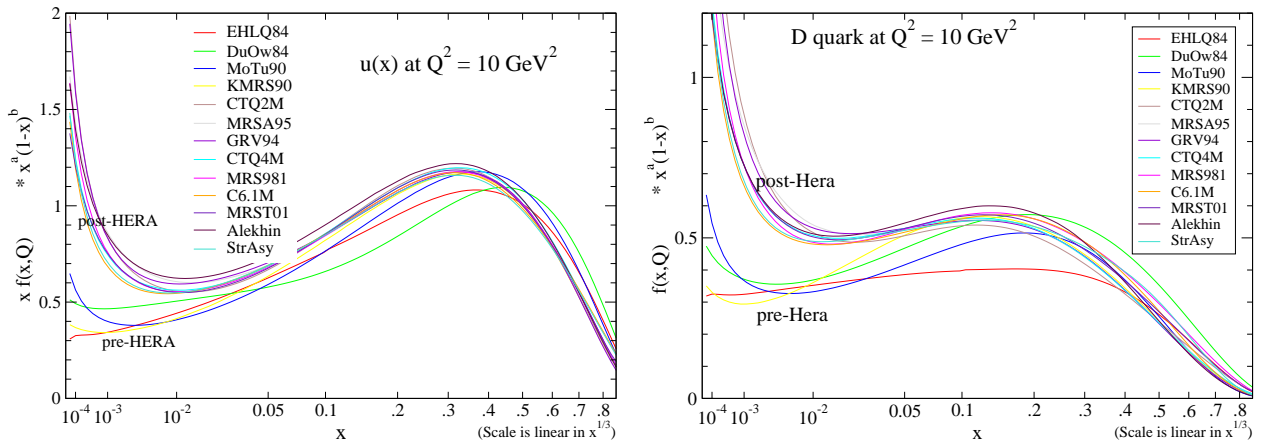


Figure 1. Historical evolution of the u quark (a) and d quark (b) distributions

years, particularly at small- x (as a direct consequence of the advent of the HERA data since the mid-1990's). Combined high precision fixed-target and HERA collider data now cover roughly the x range of $(10^{-5}, 0.75)$. These result in rather well-determined and stable u and d distributions in most recent global analyses. The remaining uncertainties concern mainly the large x behavior, beyond the measured range, particularly the d/u ratio. (Cf. Sec.3.) The discrimination between these two flavors is currently hampered by the dependence on unknown nuclear effects associated with the necessity to use DIS data on deuteron targets. (See below.)

The gluon distribution:

The historical evolution of the gluon distribution, shown in Fig.(2a), is more interesting. For reasons mentioned earlier in this section, the constraints on $g(x, Q)$ are much looser than for u and d . Hence, the first determinations of the gluon distribution varied over a wide range. The initial HERA data forced a much steeper rise of $g(x, Q)$ toward small- x , similar to the quark distributions. Notice, however, the more recent global analyses all have a much more moderate rise, or, in some cases, even a fall, in the small- x behavior of the gluon. An important contributing factor for this turn-around is the indirect effect of the inclusion of single-jet inclusive production data from the Tevatron. These data favor a larger $g(x, Q)$ at high- x , which

takes away gluons at small- x because of the overall momentum sum rule! The range over which the gluon distribution has developed over these years shows vividly both how global QCD analysis has been evolving, and how much further we need to go to determining the parton structure of the nucleon with confidence.

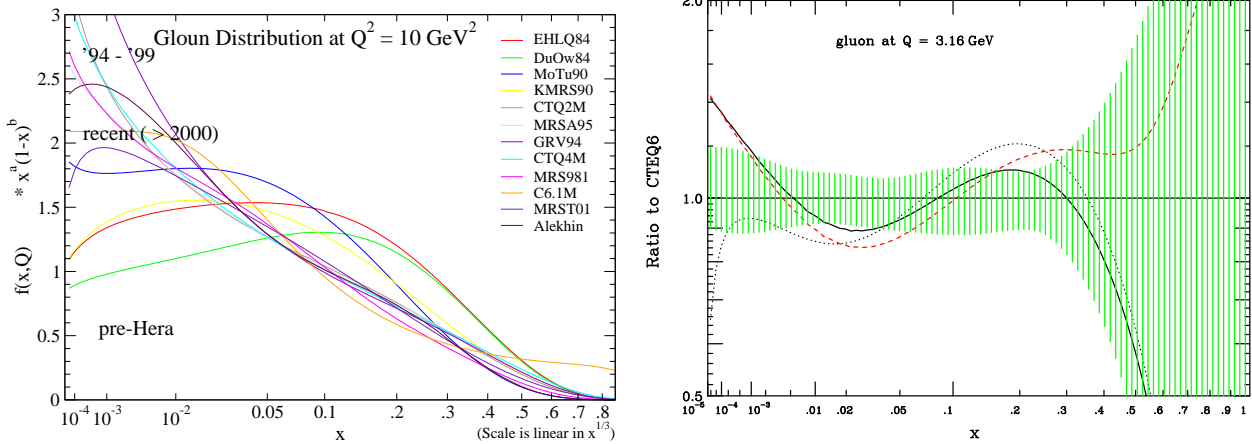


Figure 2. (a) Historical evolution of the gluon distribution; and (b) current range of uncertainty of the gluon distribution estimated by CTEQ.

The last point is reinforced by Fig.(2b), which shows the current uncertainty of the gluon distribution (due to experimental input only) estimated by the CTEQ analysis [3]. (Cf. Sec.3.) The fractional uncertainty is largest at high x , where experimental constraints are scarce. At small x , the theoretical uncertainty, not included in this plot, should be much larger than the band shown here. In fact, for certain choices of scheme and parametrization, the possibility of having negative gluons has even been raised [4]. This will be discussed in Sec.3.

The d to u ratio: The differentiation between d and u quarks relies on the difference between their couplings in neutral current and charged current interactions, and on comparing data on lepton-proton and lepton-deuteron scattering experiments. The behavior of the ratio $R_{d/u} = d(x, Q)/u(x, Q)$ as a function of x at $Q^2 = 10 \text{ GeV}^2$ is shown in Fig.(3a). The small- x region (say, $x < 0.1$) is dominated by the sea quarks. This will be discussed in the next subsection. The larger- x region ($x > 0.1$) is dominated by the valence quarks, the integral of which must be in the ratio 1 : 2, reflecting the quark number sum rule for the proton. We see that, aside from the very early PDF sets, which had no experimental constraints, d/u is relatively well-determined in the region 0.1 - 0.3. The possible range of variation of this ratio as $x \rightarrow 1$ is considerable—it is even wider than that shown in this plot, because all curves on this plot result from parametrizations of the PDFs with similar prejudices with respect to the $x \rightarrow 1$ behavior. A systematic study of the “theoretical uncertainties” has not yet been done.

Flavor Asymmetry of non-strange sea quarks: $\bar{d}-\bar{u}$

From purely perturbative considerations, early work assumed that sea quarks are flavor-independent, broken perhaps only by quark mass effects. This suggested the ansatz $\bar{u}(x, Q) = \bar{d}(x, Q)$ as an initial condition for QCD evolution. Experimental results soon proved that this conjecture is not correct. Non-perturbative physics at the confinement scale is far more subtle. The isospin asymmetry of the sea, as measured by $R_{\bar{d}\bar{u}} = \frac{\bar{d}(x, Q) - \bar{u}(x, Q)}{\bar{d}(x, Q) + \bar{u}(x, Q)}$ at $Q^2 = 10 \text{ GeV}^2$, is shown in Fig.(3b) for the same historical PDF sets as before. Some very early ones assumed $R = 0$, hence lie on the x-axis of the plot. Subsequent ones, with input from lepton-proton and lepton-deuteron scattering experiments (mainly in the small- x region that is sensitive to the sea quarks), correspond to curves that stay on the upper half plane. It turned out, however, the large- x rise was only a consequence of extrapolation. After the measurement of the ratio of DY cross sections, σ_{pD}/σ_{pp} , became available, particularly from the E866 experiment at Fermilab, the ratio R was found to turn around and decrease with x beyond $x = 0.2$. This plot again underlines the importance of

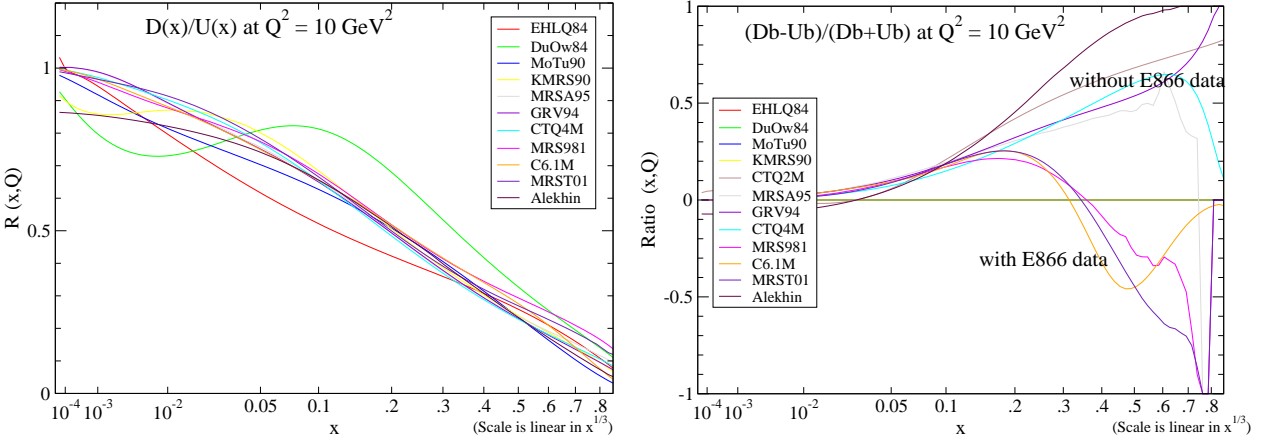


Figure 3. (a) The $d(x, Q)$ to $u(x, Q)$ ratio as a function of x ; and (b) The asymmetry between the non-strange light sea quarks \bar{d} and \bar{u} .

having the most relevant experimental constraints for each feature of the non-perturbative PDFs. Without all the necessary experimental input, even the most sophisticated analysis can yield quite unphysical results, as is illustrated by the top curve (black) obtained by Alekhin in a NNLO analysis [5] that does not include DY data.

Flavor SU(3) Asymmetry of sea quarks: strange vs. non-strange: The “naive” expectation of flavor SU(3) symmetry, $s = \bar{s} = \bar{d} = \bar{u}$, assumed in some early PDF studies, is clearly unrealistic: the strange quark mass alone would induce a difference between (s, \bar{s}) and, say, $(\bar{u} + \bar{d})/2$. As mentioned earlier, experimental evidence suggests that the ratio $R_{s+} \equiv \frac{s+s}{\bar{u}+\bar{d}}$, is of the order 0.5 at a scale of 1-2 GeV. Up to now, this ratio is mainly enforced as a constraint in global analyses, rather than as the result of actual fitting to data, because the relevant data have not been presented in a form suitable for global analysis. We show the actual values of R_{s+} for the various PDF sets seen on this plot is more due to the minor variation on how and where the condition $R_{s+} \sim 0.5$ is implemented, rather than on hard experimental input. Thus, there is no regular pattern in terms of the historical development (other than the departure from the naive perturbative $R_{s+} = 1$ assumption).

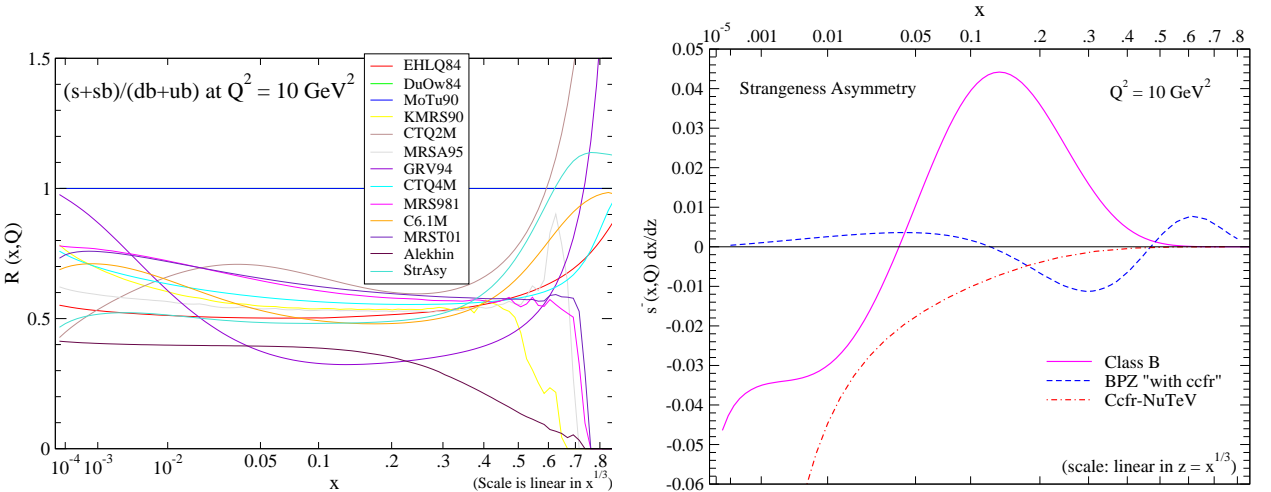


Figure 4. (a) The asymmetry between the strange and the light non-strange sea quarks; and (b) The strangeness asymmetry as a function of x : shown are results from a recent global analysis, along with two earlier results cf. [6] for explanation.

Strangeness Charge Asymmetry: In the absence of any strong theoretical argument or experimental evidence to the contrary, the strange and anti-strange quark distributions, $s(x, Q)$ and $\bar{s}(x, Q)$, have traditionally been assumed to be equal to each other in all widely available PDFs. Recent developments, particularly in relation to the NuTeV anomaly, have motivated a re-examination of this assumption. In a phenomenological study performed in the global analysis context [6], analysis of the CCFR-NuTeV data on dimuon (charm) production in neutrino and anti-neutrino scattering gave preliminary evidence of a positive non-perturbative strangeness asymmetry in terms of the first moment integral $[S^-] \equiv \int_0^1 x[s(x) - \bar{s}(x)]dx$. In Fig.(4b), we show the result of this analysis, along with earlier results that have known problems. (See [6].) From perturbation theory, it has been pointed out that the 3-loop QCD evolution kernel generates a non-zero (negative) strangeness asymmetry, even if one starts with a symmetric non-perturbative input to the analysis. The situation is clearly unsettled at the moment.

Possible Isospin Violation in the Parton Structure of the Nucleon: Interest in possible explanations of the NuTeV anomaly has also motivated the study of the possibility that $u_{\text{proton}}(x, Q) \neq d_{\text{neutron}}(x, Q)$. Experimental constraints on this effect are very weak, even without taking into account the large uncertainties about nuclear corrections that are needed to measure neutron structure functions [4]. Theoretically, it has been pointed out that isospin violation in PDFs arises naturally when one tries to include electroweak corrections in the global QCD analysis: the evolution equations of PDFs will then include photon distributions of the nucleon; $u_{\text{proton}}(x, Q)$ and $d_{\text{neutron}}(x, Q)$ distributions will evolve differently due to their different electric charge. This effect has been studied; it is small, as expected.

Heavy Quark distributions—Charm and Bottom: Although there has been much discussion about the physical processes involving heavy quark production in the literature, there is as yet not very much reliable information on the heavy flavor parton distributions. Of the heavy quarks c , b , and t , only the c and b quark-partons participate actively in PQCD calculations of high energy processes for physical processes at energy scales even up to LHC. The definition of heavy quark partons is even more scheme-dependent than that of light quark flavors. In the so-called (fixed) 3-flavor scheme, there are, by definition, no heavy quark partons at all; whereas in the (fixed) 4-flavor scheme, there is a charm distribution, but no bottom distribution. These schemes are of use only for limited energy ranges. In recent years, a consensus has emerged that the variable-flavor number scheme, which is a generalization of the conventional msbar zero-mass parton scheme, is the appropriate one to use for calculations that cover a wide range of Q . If one assumes that there is no non-perturbative heavy flavor content in the nucleon, then heavy flavor parton distribution functions c and b are “radiatively generated” by QCD evolution from their respective thresholds. This is the assumption used in practically all existing global analyses of PDFs. Unfortunately, the concept of radiatively generated heavy quark partons is not well-defined, since the location of “heavy quark threshold” for a given flavor is itself ambiguous: it can be any value of the same order of magnitude as the heavy quark mass or the physical heavy flavor particles.

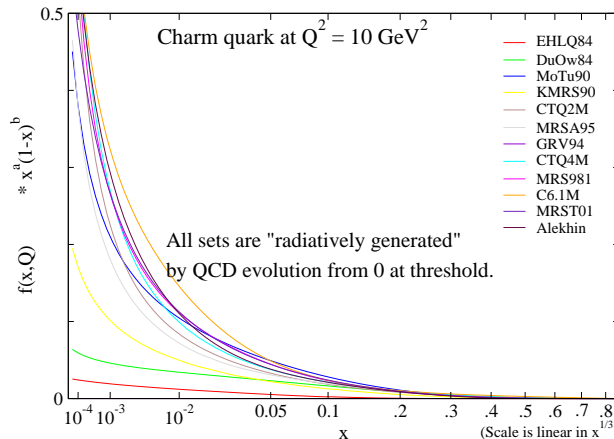


Figure 5. (a) The charm distribution function.

Fig.(5) shows the charm distribution at $Q^2 = 10 \text{ GeV}^2$ for the various PDF sets. The small- x behavior of the radiatively generated distribution has changed rather dramatically over time, mainly as the indirect consequence of the change of small- x behavior of the light partons, driven by the HERA data. For reasons mentioned above, the actual behavior of $c(x, Q)$ remains largely unexplored. Both new data and new theoretical assumptions could change these results rather drastically.

2 Open Issues in Global QCD Analysis

The above survey of various aspects of the parton structure of the nucleon amply illustrates that, although a lot of progress has been made over the last 20 years, many features of the PDFs still are uncertain, or unknown. These open issues are summarized here.

- The gluon distribution: both the small x and large- x behavior of the gluon distribution $g(x, Q)$ are still subject to large uncertainties. Two current results are worth further investigation.
 - ◊ The MRST global analysis favors a negative gluon at small- x at a momentum scale of $1 \text{ GeV} < Q < 2 \text{ GeV}$. Is this “required” by current experimental input? Is this behavior “natural” theoretically?
 - ◊ The CTEQ6 gluon distributions at large x are higher than in most other PDF sets; $g(x, Q_0)$ falls off as $(1 - x)^\alpha$ with a power α that is slightly smaller than the power for the valence quark. This is driven by the inclusive jet data used in the analysis. But is it theoretically “natural”?
- The $R_{d/u}$ ratio: should this ratio approach 0, $\frac{1}{4}$, $\frac{3}{7}$, or some other number, as $x \rightarrow 1$? How do we determine the large- x behavior of this ratio phenomenologically? Is there a reliable way to apply deuteron corrections to data obtained with deuteron target, which can significantly affect the analysis?
- The strange quark distribution: the strangeness sector of PDFs is most conveniently studied in terms of $s_\pm = s \pm \bar{s}$, which correspond to different quantum numbers, and embody different underlying physics.
 - ◊ The symmetric combination $s_+(x, Q)$ is easier to study since it can be probed by charm production in DIS experiments using combined neutrino and anti-neutrino beams. After many years of effort, however, the uncertainty on s_+ is still quite large. For instance, aside from the relative suppression of strange compared to non-strange sea, we cannot yet be certain whether $s_+(x, Q_0)$ can be sufficiently represented by the same functional form as, say $\bar{u}(x, Q_0) + \bar{d}(x, Q_0)$, with only a normalization factor κ . A detailed NLO global analysis, including the recent CCFR-NuTeV dimuon production data, can possibly yield an improved knowledge on $R_{s+}(x, Q) \equiv \frac{s+s}{\bar{u}+\bar{d}}$, including a quantitative estimate of the uncertainties. This remains to be carried out.
 - ◊ The antisymmetric combination $s_-(x, Q) = s(x, Q) - \bar{s}(x, Q)$ is harder to determine, because it requires the measurement of the difference between neutrino and anti-neutrino cross sections with charm final states. The status of this determination was briefly discussed in the previous section. (Cf. Ref.[6]) In practice, it is convenient to parametrize the ratio $R_{\text{StrAsy}}(x, Q_0) \equiv \frac{s(x) - \bar{s}(x)}{s(x) + \bar{s}(x)}|_{Q_0}$ which must satisfy the constraint $|R_{\text{StrAsy}}| \leq 1$ in order to ensure positivity of the distributions s and \bar{s} . A full NLO global analysis of this quantity is also currently underway, in conjunction with the s_+ study described above.
- Isospin Violation in the Parton Structure of the Nucleon:
(See the previous section.)
- Heavy Quark Distributions: (See the previous section.)

3 Uncertainties of Parton Distributions

In parallel with the determination of ever improving “best-fit” PDFs, an equally important front in global analysis has been opened in recent years—the development of quantifiable uncertainties on the PDFs and their physical predictions. Several groups have carried out extensive studies with different techniques and emphases. Much progress has been made; many useful results have been obtained; but there are, as yet, no unambiguous conclusions. The basic problem lies with the complexity of the global analysis that (i) utilizes results from many experiments on a variety of physical processes, with diverse characteristics and errors, and often not mutually compatible according to textbook statistics; (ii) may be sensitive to many theoretical uncertainties that cannot yet be quantified; and (iii) can depend on the choice of parametrization of the non-perturbative functions used in the analysis. Individually and collectively, these factors render a *rigorous* approach to error analysis untenable.

As an illustration of point (i), we briefly describe results on a study of the uncertainty of the W production

cross section at the Tevatron due to known experimental errors on the input data sets, conducted by the CTEQ group [3] using the Lagrange Multiplier method they proposed. First, we obtain a series of PDFs that provide best fits to the global data, but constrained to yield a range of possible values of σ_W at the Tevatron around the CTEQ6M value (which corresponds to the least overall χ^2 by definition). Then, we evaluate the individual χ^2 of each experimental data set to gauge the consistency between the data sets, as well as to assess sensible ways to quantify the overall uncertainty of the prediction on σ_W due to the input experimental uncertainties. The results are shown in the two plots of Fig.(6). The horizontal axes

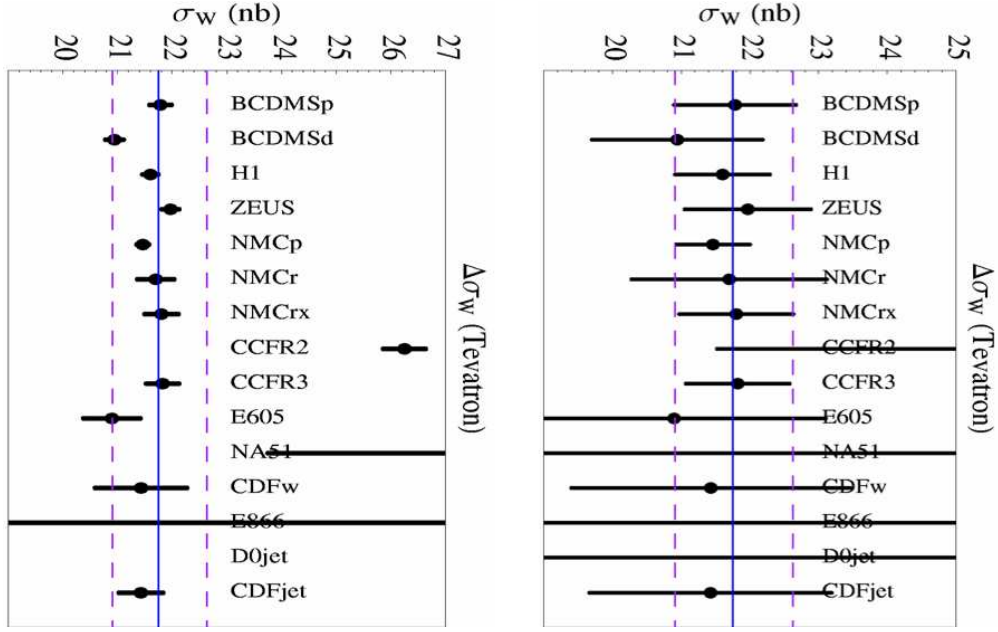


Figure 6. Predicted value of σ_W at the Tevatron: (a) $\Delta\chi^2 = 1$ error ranges for individual experimental data sets evaluated from PDF sets obtained by the Lagrange Multiplier method in constrained global fits; and (b) 90% confidence level ranges for the same data sets and PDF sets.

correspond to the values of σ_W . For each of the 15 input experimental data sets, a best-fit value and a range is shown. These are arranged vertically, in no particular order. On the left plot, each range corresponds to a $\Delta\chi^2 = 1$ error due to that experiment; while on the right plot, it corresponds to a “90% confidence level” (cumulative distribution function of the χ^2 normalized to the best fit). We see clearly: (i) if a $\Delta\chi^2 = 1$ error criterion is strictly enforced, then there is no common value for the predicted σ_W (or, equivalently, some of the data sets must be deemed mutually incompatible); but (ii) within the 90% confidence level range, there is a common range for σ_W that spans the values indicated by the dashed vertical lines.

Faced with the problem of nominally incompatible data sets (which is common in combined analysis of data from diverse experiments, e.g. PDG work), subjective assumptions and compromise measures are necessary to obtain sensible results. Several approaches have been followed by the different global analysis groups. CTEQ uses the ansatz that the range of uncertainty indicated in Fig.(6b) represents a 90% C.L. uncertainty on σ_W ; and, in general, characterizes the PDF uncertainties by using similar criteria along 20 orthonormal eigenvector directions in the PDF parameter space, using an improved Hessian method.^a MRST has adopted the same approach [7], albeit choosing a slightly narrower range of the uncertainty. The H1 and ZEUS PDF analysis groups also adopt similar methods, but, by restricting the input data sets to DIS experiments only, apply their own definition of the range. [8] The important fact is that these different groups (all using the leading twist PQCD formalism) arrive at quite comparable results, both for the PDFs and for the magnitude of the error bands, even if some details are different because of the variations in experimental and theoretical inputs.

^aIn terms of the total χ^2 of the global data sets, consisting of ~ 2000 data points in current analysis, this range corresponds to $\Delta\chi^2 \sim 100$. There is no a priori significance to this number, since the global χ^2 used in this context only represents a broad measure of goodness-of-fit; it does not have rigorous statistical significance. As data increase in quantity and quality, the equivalent $\Delta\chi^2$ value will change. Similarly, when applied to a different observable or set of input data, the number will vary.

With this approach, both CTEQ and MRST have been able to make estimates on future measurements. Two examples are given in Fig.(7). Fig.(7a) shows fractional uncertainties in the predicted $q\bar{q}$ and GG

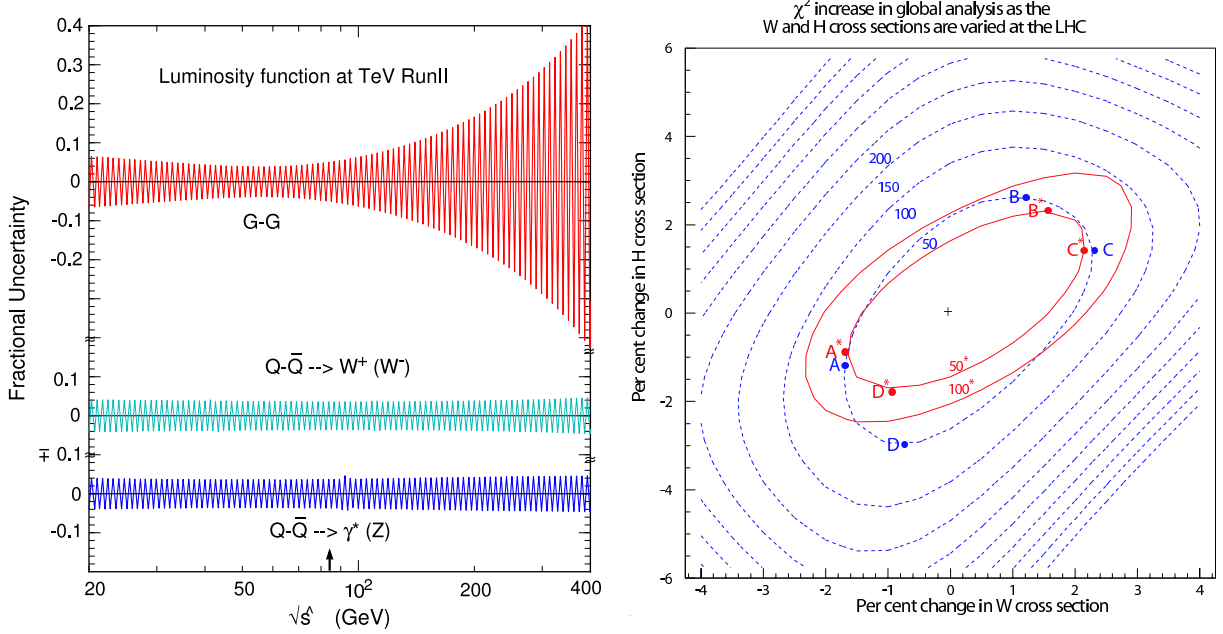


Figure 7. Examples of ranges of predictions at Tevatron Run II and LHC associated with uncertainties of PDFs due to experimental input. See text.

parton luminosity functions as a function of \sqrt{s} at the Tevatron energy obtained by CTEQ, from which the values and the uncertainty ranges of a variety of physical processes, both in the SM and beyond, can be obtained. We see the considerable uncertainties associated with the gluon-gluon luminosity at large x . Fig.(7b) shows contours of increasing χ^2 in the σ_W - σ_H plane due to PDF uncertainties at LHC obtained by MRST. Theoretical uncertainties are not included in either plot.

A different approach is followed by Alekhin [5]. The experimental input is restricted to DIS experiments only, and the theoretical framework is broadened to include higher-twist effects, among others, in order to better accommodate the different data sets. A consistent fit is then achieved in the strict statistical sense; and the uncertainty range is defined according to the classic $\Delta\chi^2 = 1$ criterion. However, by forgoing the critical experimental constraints provided by Drell-Yan and inclusive jet production data, the determination of the PDFs can not be complete. Applying the Alekhin PDFs to the available DY data sets (E605, CDF W-asymmetry, E866), one obtains a χ^2 of 892 for 145 data points—a clear indication that vital information is missing on certain aspects of PDFs. This can be seen in the plot of $\frac{\bar{d}-\bar{u}}{d+\bar{u}}$ shown in Fig.(3b), where the Alekhin curve is similar to earlier PDFs that did not include DY asymmetry data sets, but is completely different from other modern PDFs that do fit the DY data. Under these circumstances, one might ask, what is the use of these PDF uncertainties defined by the textbook $\Delta\chi^2 = 1$ rule? Giele *et al* [9] also emphasize a rigorous statistical approach, using the more general likelihood method. Within the leading twist PQCD approach, this leads to acceptable results only if one restricts the input experimental data sets to one or few DIS sets. Thus, depending on which subsets of data are used, one gets many predictions on physical quantities (such as σ_W) with “ 1σ -error” ranges, which do not overlap with each other. This leaves unanswered the important question: “What is the best estimate of current uncertainty, given all available experiments?”.

Thus, the underlying facts seen by all groups are consistent with each other; the differences lie in the emphases placed to cope with these facts. In principle, all methods are equivalent: in an ideal world where all experiments came up with textbook-like errors, they would yield the same results. In reality, in the complex world of global analysis, the results appear different or non-existent (if strict criteria are applied), depending on subjective judgements made in placing the emphases. This state of affairs requires the users of PDFs to be well-informed about the nature of the “uncertainties” provided by the various global analysis

groups; and then to use these judiciously according to their own (subjective) judgement. Unfortunate it may be, but there is no “ $1\text{-}\sigma$ PDF error” that can be defended scientifically on all accounts. This points to the need for continued hard work, both on the experimental and theoretical fronts, in order to improve the situation, and to reduce the ambiguities described above. To this end, the physics programs of HERA II, Tevatron Run II, as well as several fixed-target experiments, can make important contributions in the immediate future. Through these efforts, the PDFs and their uncertainties will certainly be better known when the LHC comes on line. This will lead to better predictions on both SM and new physics processes, hence improve the potential for all discoveries. In addition, the high reaches of LHC, both in energy range and in statistics, will provide additional constraints on PDFs, hence allow even better determination of the parton structure of the nucleon.

4 Other important topics relating to global analysis

Due to space limitation, many areas of active work relevant for global QCD analysis cannot be included in this survey. These include: (i) the completion of the NNLO (3-loop) calculation of the QCD evolution kernel; (ii) important advances in the calculation of NLO and NNLO hard cross sections for a variety of physical processes; (iii) inclusion of electroweak effects in the QCD global analysis; (iv) estimates of theoretical uncertainties, with implications on the stability of the NLO global analysis; and many more. They are covered elsewhere in the proceedings, either in the parallel sessions or in the concluding plenary sessions.

Acknowledgements

Much of the material reported in this review is based on CTEQ work, particularly in collaboration with my MSU colleagues Joey Huston, Jon Pumplin and Dan Stump, and on published results of other QCD analysis groups. The perspectives expressed here are borne out of fruitful discussions with members of CTEQ, MRST, the PDF analysis groups of H1 and ZEUS, S. Alekhin, W. Giele, and many others in the global QCD analysis community.

References

1. D. W. Duke and J. F. Owens, Phys. Rev. D **30**, 49 (1984).
2. E. Eichten, I. Hinchliffe, K. D. Lane and C. Quigg, Rev. Mod. Phys. **56**, 579 (1984) [Addendum-ibid. **58**, 1065 (1986)].
3. J. Pumplin, D. R. Stump, J. Huston, H. L. Lai, P. Nadolsky and W. K. Tung, JHEP **0207**, 012 (2002) [arXiv:hep-ph/0201195], and references therein.
4. A. D. Martin, R. G. Roberts, W. J. Stirling and R. S. Thorne, Eur. Phys. J. C **35**, 325 (2004) [arXiv:hep-ph/0308087].
5. S. Alekhin, Phys. Rev. D **68**, 014002 (2003) [arXiv:hep-ph/0211096], and references therein.
6. S. Kretzer, F. Olness, J. Pumplin, D. Stump, W. K. Tung and M. H. Reno, Phys. Rev. Lett. **93**, 041802 (2004) [arXiv:hep-ph/0312322]; F. Olness *et al.*, arXiv:hep-ph/0312323.
7. A. D. Martin, R. G. Roberts, W. J. Stirling and R. S. Thorne, Eur. Phys. J. C **28**, 455 (2003) [arXiv:hep-ph/0211080], and references therein.
8. A. M. Cooper-Sarkar, J. Phys. G **28**, 2669 (2002) [arXiv:hep-ph/0205153];
also <http://www-zeuthen.desy.de/~moch/heralhc/gwenlan-coopersarkar.pdf>
9. W. T. Giele and S. Keller, Phys. Rev. D **58**, 094023 (1998) [arXiv:hep-ph/9803393]; W. T. Giele, S. A. Keller and D. A. Kosower, arXiv:hep-ph/0104052 (unpublished).